

## Surface Analysis of Wall Samples Exposed to LHD Plasmas in the Starting Phase

INOUE Noriyuki\*, SAGARA Akio, NODA Nobuaki, HIROHATA Yuko<sup>1</sup>,  
HINO Tomoaki<sup>1</sup>, MORITA Kenji<sup>2</sup>, YOSHIDA Naoaki<sup>3</sup> and MOTOJIMA Osamu

*National Institute for Fusion Science, Toki 509-5292, JAPAN*

<sup>1</sup>*Hokkaido University, Kita, Sapporo 060-0813, JAPAN*

<sup>2</sup>*Nagoya University, Chikusa, Nagoya 464-8601, JAPAN*

<sup>3</sup>*Kyushu University, Kasuga, Fukuoka 816-8580, JAPAN*

(Received: 18 January 2000 / Accepted: 28 September 2000)

### Abstract

In the starting phase of LHD, the deposited elements on the first wall and divertor were analyzed by using surface probe samples made of stainless steel and graphite. After finishing the first campaign and opening the vessel to air, surface samples have been analyzed using SEM, RBS, AES and EDS. There were observed deposited thin films which mainly consist of O and Fe. The deposition of Fe impurity was presumed to be generated by the sputtering of wall materials due to charge exchange fast neutral particles, or redeposition of sputtered impurities by ion impact at the divertor striking point. There was not detected any titanium elements on the sample near the location of Ti sublimation head, suggesting that the metal impurities were not moved for a long distance by sputtering and redeposition. The large amount of deposited impurities at the divertor striking point was attributed to their flow to the divertor through SOL.

### Keywords:

plasma wall interaction, surface probe, RBS, LHD, first wall, divertor, redeposition

### 1. Introduction

In the first campaign of Large Helical Device (LHD), the deposited elements on the first wall and divertor were analyzed by using surface probe samples. LHD was successfully started up with discharge cleaning without high temperature baking [1]. After finishing the first campaign and opening the vessel to air, samples were analyzed using the SEM, RBS, AES and EDS. The deposited impurities on samples at several points on the first wall were discussed relating to each location such as the distance from core plasma, divertor plasma and a titanium sublimation head.

LHD is a superconducting toroidal device with a continuous helical divertor as a plasma edge control

tool. The impurity distribution at the divertor striking point was measured on the graphite sample whose surface was perpendicular to the divertor plasma.

### 2. Experimental

#### 2.1 Vacuum vessel of LHD

The vacuum vessel ( $R = 3.9$  m,  $r = 1.6$  m) has a dumbbell-shaped cross section (see Fig. 1). It is made of 316L stainless steel (SS). The total volume and the inner surface area are  $210$  m<sup>3</sup> and  $870$  m<sup>2</sup>, respectively [2]. The vacuum vessel was constructed by using a press forming and a welding. The inner surface was cleaned with acid, then with demineralized water, and finally

\*Corresponding author's e-mail: [inoue@lhd.nifs.ac.jp](mailto:inoue@lhd.nifs.ac.jp)

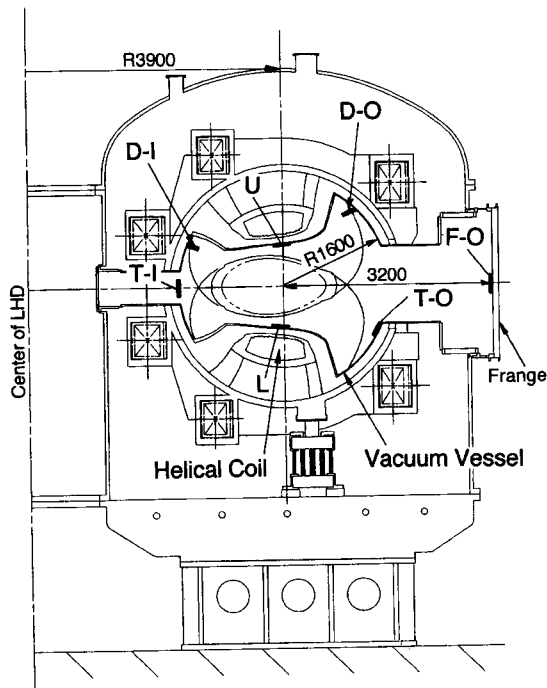


Fig. 1 Poloidal cross section of LHD vacuum vessel and locations of probe samples.

with alcohol. The maximum temperature of the vacuum vessel is limited below 373 K due to the cryogenic capability for the superconducting magnets [3].

## 2.2 Surface probes

The stainless steel and graphite (C) were used for the surface probe. The surface of vacuum vessel was not as clean as the surface treated with electrolytic polishing. To investigate the deposition on the first wall, the SS sample was made of the same material as the vacuum vessel. Figure 2(a) shows a sample holder set at the first wall for the C sample ( $\phi 25.4 \text{ mm} \times 1.6 \text{ mm}$ ) and the SS sample ( $20 \text{ mm} \times 10 \text{ mm} \times 1 \text{ mm}$ ). Five sets of the sample holders on the first wall were set in the same poloidal cross section of the vacuum vessel (see Fig. 1). Figure 2(b) shows the graphite sample plates ( $45 \text{ mm} \times 82 \text{ mm} \times 5 \text{ mm}$ ) and the supporting holder at the divertor striking point (D-I and D-O in Fig. 1). These sample holders were set on the vessel wall using spot welding. Since the divertor heat flux was not high in the first campaign, it was allowed to set the samples there. The surface was chosen to receive the flow of the divertor plasma along the magnetic field lines.

## 2.3 Wall conditioning and plasma operations

LHD has been successfully started up with

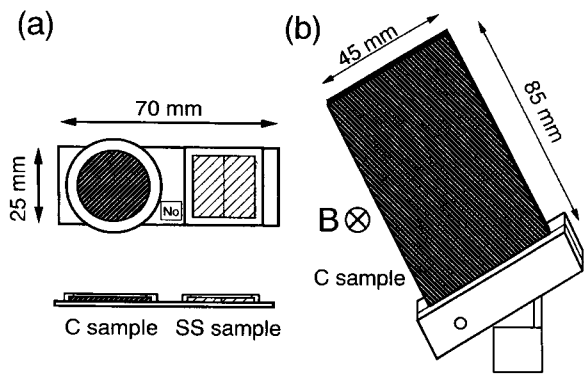


Fig. 2 Surface probe samples and holders. (a) The first wall samples of the graphite and stainless steel. (b) The divertor sample of graphite whose surface is facing to the divertor plasma.

discharge cleaning without baking at high temperatures. The details of wall conditioning at the starting phase of LHD were reported by Sagara *et al.* [1]. In the first campaign, 5 kW ECR-DC with a total duration of 380 hours and a baking at 368 K with 61 hours were performed. Titanium gettering was also conducted twice a day, with an average deposition rate of about 3 monolayers a day. The first plasma experiments were conducted with 2<sup>nd</sup> harmonic 84-GHz and 82.6-GHz ECH with a power input of 350 kW, then about 1800 main discharge shots were produced under magnetic field at 1.5 T [4]. Glow discharge was once tested but not used for cleaning in the first campaign.

Typical peak temperature  $T_e$  of 1.3 keV at ECH power of 270 kW, maximum density  $n_e$  of  $1.3 \times 10^{19} \text{ m}^{-3}$  at ECH power of 80 kW, and energy confinement time  $\tau_e$  of up to 0.25 s at  $n_e$  of  $6 \times 10^{18} \text{ m}^{-3}$  and ECH power of 70 kW were obtained in the first campaign [5]. The experiment was usually performed at a magnetic axis position R of 3.75 m.

## 3. Results and discussions

### 3.1 Divertor samples

Figure 3 shows the results of the RBS analysis on the graphite sample at the inner striking point of divertor plasma. The large amount of deposited impurities was obtained around the striking point. The detail will be discussed in elsewhere in comparison with the calculated divertor leg structure [6].

The deposition of a thin film which consists of O, Fe and Mo was observed. Iron and molybdenum were presumed to be due to redeposition of sputtered impurities from the vessel wall of stainless steel by ion

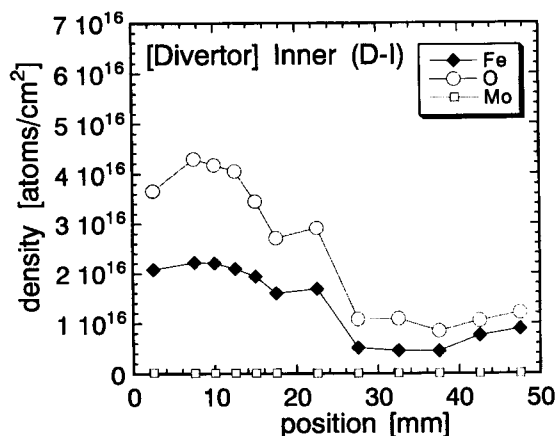


Fig. 3 Deposited impurity distributions on the graphite sample at the divertor striking point measured by RBS analysis.

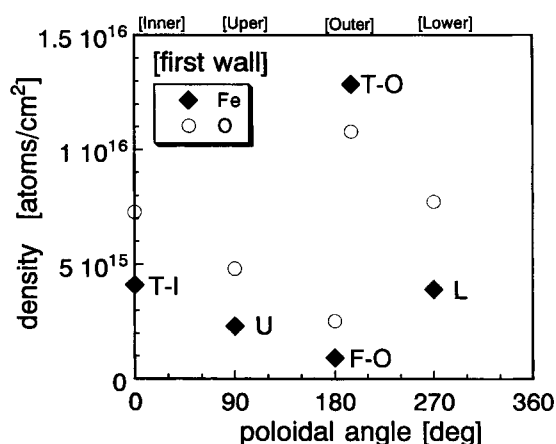


Fig. 4 Deposited impurity distributions with poloidal angle on the graphite sample at the first wall measured by RBS analysis.

impact at the striking point of divertor plasma, or by charge exchange fast neutrals from core plasma. On the backside surface of the sample, the impurity deposition was also detected, which was mainly due to redeposition of sputtered impurities by divertor plasma.

### 3.2 First wall samples

The poloidal distributions of impurity amount were analyzed on the graphite samples at the first wall by RBS analysis. Main elements observed on the surface were Fe and O with base material of graphite. On the stainless steel samples, carbon element was not clearly detected above a noise level on the Fe signal. As shown in Fig. 4, there is no significant difference on the

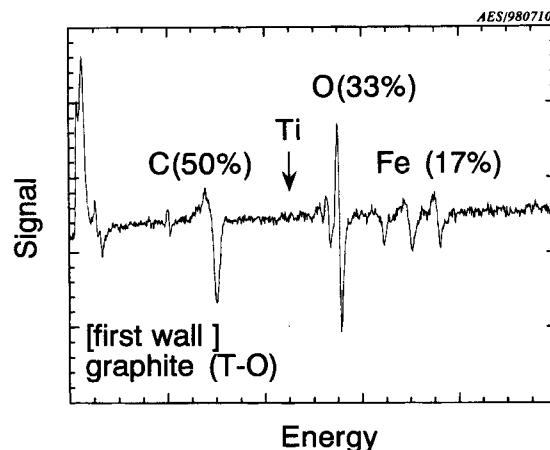


Fig. 5 AES analysis on the graphite sample at the first wall which was located at the 1.25 helical pitch away from the nearest  $T_i$  sublimation head.

impurity amount between U and L. On the other hand, T-O and F-O shows a large difference even at the almost same poloidal angle. The details will be discussed in the next section from the point of view of distance from core plasma.

The sample was located at the 1.25 helical pitch away from the nearest  $T_i$  sublimation head. The sample does not see the  $T_i$  sublimation head directly. As shown in Fig. 5, titanium element is not detected with AES as well as RBS. Therefore, this result suggests that these detected metals were not moved for a long distance by sputtering and redeposition.

### 3.3 Discussions

Origin of the deposited iron element is the stainless steel of the vacuum vessel. The ions of higher impact energy than the sputtering threshold are hardly produced by ECR-DC ( $T_i, T_e < 5$  eV), and GDC was not used for discharge cleaning in the first campaign. Therefore, the metal impurities are attributed to sputtering of the first wall mainly due to charge exchange fast neutrals during ECH main discharges. The mean free path of fast neutrals was estimated as approximately 5 cm using diagnostics data in second campaign. Typical ion temperature of the ECH plasmas was measured to be higher than 300 eV, which suggests that significant neutral flux is emitted above the threshold energy, 90 eV for H and 25 eV for He, of sputtering of iron.

It is expected that the flux of charge exchange fast neutrals depends on the distance from the core plasma. The distance from the plasma center was about 0.67 m at U and L, 1.6 m at T-I and T-O, and 3.2 m at F-O.

Figure 6 shows the change of impurity amount as a function of the distance from core plasma. The impurity amount at the outer torus position (T-O) is 3 times as large as that of the inner position (T-I). And the impurity amount of T-I and T-O are larger than that of U and L. Since these samples were located near the divertor legs, the difference of impurity amount may be due to the difference of the distance and the direction from each striking point of divertor plasma.

The lowest amount of Fe impurity is found at outer flange (F-O), which is farthest position from the core plasma. The thermal desorption spectroscopy (TDS) analysis on the same sample position has been reported by Hino *et al.* [7]. The helium gas desorption is detected only a little at F-O, where the helium gas was used for the main plasma experiment.

Figure 7 shows the relationship between the amount of deposited Fe and O at the first wall and divertor. Since these samples were exposed to air before analysis, oxidation of Fe, such as  $Fe_2O_3$ , should be partly taken into account. At the divertor position, the total amount of impurities is larger than that of other positions. This result suggests that impurity ions are transported through the scrape-off layer (SOL) into the divertor region, especially to the divertor striking points.

#### 4. Conclusion

The deposition of a thin film which mainly consists of oxygen and iron was observed on the surface probe samples in LHD. Metal impurities were presumed to be due to redeposition of sputtered impurities from the vessel wall of stainless steel by charge exchanged fast neutrals or by ion impact at the divertor striking point. There was not detected any  $T_i$  elements on the sample near the  $T_i$  sublimation head, suggesting that the metal impurities were not moved for a long distance by sputtering and redeposition. The large amount of deposit impurities at the divertor position was attributed to the divertor function of impurity removal.

In the future campaigns, the probe samples are set again to study the surface modification of the wall under higher plasma performance and additional conditioning methods such as glow discharge cleaning and bolonization.

#### Acknowledgements

The authors are grateful to Dr. J. Yuhara and Dr. K. Tsuzuki, for useful discussions and help on RBS analysis in Nagoya University.

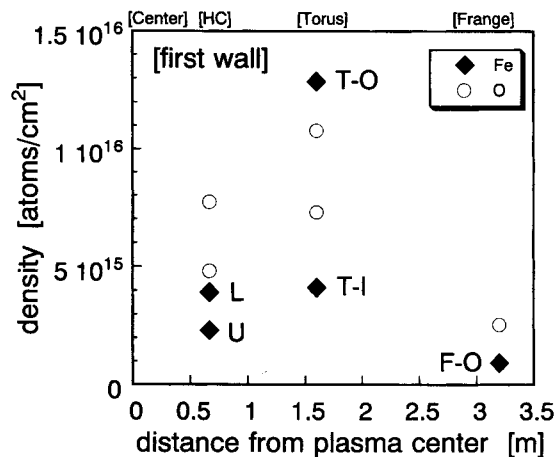


Fig. 6 Change of deposited impurity densities with the distance from plasma center. The data are replotted from Fig. 4.

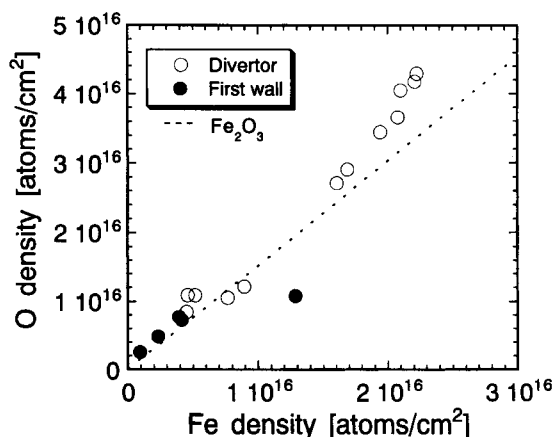


Fig. 7 The relationship between iron density and oxygen density on graphite samples at the first wall and divertor. The data were replotted from Figs. 3 and 4.

#### References

- [1] A. Sagara *et al.*, J. Plasma and Fusion Research 75 3, 263-267 (1999).
- [2] N. Inoue *et al.*, Fusion Eng. Des. 41, 331-336 (1998).
- [3] O. Motojima *et al.*, Nucl. Fusion 40 3Y, 599-609 (2000).
- [4] M. Fujiwara *et al.*, Nucl. Fusion 39 11Y, 1659-1666 (1999).
- [5] A. Iiyoshi *et al.*, 39 9Y, 1245-1256 (1999).
- [6] T. Morisaki, Annual Report of National Institute for Fusion Science 1997-1998, 47 (1998).
- [7] T. Hino *et al.*, to be published in J. Nucl. Mater.